

ORIGINAL ARTICLE

Open Access



Visual and quantitative assessment of hip implant-related metal artifacts at low field MRI: a phantom study comparing a 0.55-T system with 1.5-T and 3-T systems

Hanns-Christian Breit¹, Jan Vosshenrich^{1*} , Martin Clauss², Thomas J. Weikert¹, Bram Stieltjes¹, Balázs K. Kovacs¹, Michael Bach¹ and Dorothee Harder¹

Abstract

Background To investigate hip implant-related metal artifacts on a 0.55-T system compared with 1.5-T and 3-T systems.

Methods Total hip arthroplasty made of three different alloys were evaluated in a water phantom at 0.55, 1.5, and 3 T using routine protocols. Visually assessment (VA) was performed by three readers using a Likert scale from 0 (no artifacts) to 6 (extremely severe artifacts). Quantitative assessment (QA) was performed using the coefficient of variation (CoV) and the fraction of voxels within a threshold of the mean signal intensity compared to an automatically defined region of interest (FVwT). Agreement was evaluated using intra/inter-class correlation coefficient (ICC).

Results Interreader agreement of VA was strong-to-moderate (ICC 0.74–0.82). At all field strengths (0.55-T/1.5-T/3-T), artifacts were assigned a lower score for titanium (Ti) alloys (2.44/2.9/2.7) than for stainless steel (Fe-Cr) (4.1/3.9/5.1) and cobalt-chromium (Co-Cr) alloys (4.1/4.1/5.2) ($p < 0.001$ for both). Artifacts were lower for 0.55-T and 1.5-T than for 3-T systems, for all implants ($p \leq 0.049$). A strong VA-to-QA correlation was found ($r = 0.81$; $p < 0.001$); CoV was lower for Ti alloys than for Fe-Cr and Co-Cr alloys at all field strengths. The FVwT showed a negative correlation with VA ($-0.68 < r < -0.84$; $p < 0.001$).

Conclusions Artifact intensity was lowest for Ti alloys at 0.55 T. For other alloys, it was similar at 0.55 T and 1.5 T, higher at 3 T. Despite an inferior gradient system and a larger bore width, the 0.55-T system showed the same artifact intensity of the 1.5-T system.

Keywords Artifacts, Titanium, Hip prosthesis, Image processing (computer-assisted), Magnetic resonance imaging

Key points

- Low field magnetic resonance imaging (MRI) currently experiences a renaissance.
- Low field (0.55 T) MRI resulted to be equal to 1.5-T MRI in terms of artifact reduction, even with a weaker gradient system and larger bore size.
- 3-T MRI resulted to be inferior to 1.5-T and 0.55-T MRI in terms of artifact reduction for standard alloys hip implants

*Correspondence:

Jan Vosshenrich
jan.vosshenrich@usb.ch

¹ Department of Radiology, University Hospital Basel, Petersgraben 4, 4031 Basel, Switzerland

² Department of Orthopaedics and Traumatology, |University Hospital Basel, Spitalstrasse 21, 4031 Basel, Switzerland



© The Author(s) 2023. **Open Access** This article is licensed under a Creative Commons Attribution 4.0 International License, which permits use, sharing, adaptation, distribution and reproduction in any medium or format, as long as you give appropriate credit to the original author(s) and the source, provide a link to the Creative Commons licence, and indicate if changes were made. The images or other third party material in this article are included in the article's Creative Commons licence, unless indicated otherwise in a credit line to the material. If material is not included in the article's Creative Commons licence and your intended use is not permitted by statutory regulation or exceeds the permitted use, you will need to obtain permission directly from the copyright holder. To view a copy of this licence, visit <http://creativecommons.org/licenses/by/4.0/>.

Background

Worldwide demand for total hip arthroplasty continuously increases and is projected to multiply within the next years [1, 2]. Especially in younger patients of less than 65 years of age, this trend will probably cause a similar rise in revision surgery, given artificial hips' limited lifetime [3, 4]. As a consequence, also the need for magnetic resonance imaging (MRI) in this population, *e.g.*, to assess complications such as implant failure or loosening [5] as well as pathologies in the surrounding soft tissues [6], will likely increase to a certain extent.

The diagnostic capabilities of MRI have been proven to be superior to ultrasound and computed tomography in this setting, especially when aiming to detect and quantify muscle atrophy, pseudotumors, and other soft tissue changes [7–9]. This further emphasizes the key role of MRI in future imaging musculoskeletal diagnostic pathways.

Traditionally, MRI of metal implants has been challenging due to susceptibility-induced artifacts, degrading image quality and diagnostic accuracy. Extensive research in the fields of protocol optimization and metal artifact reduction techniques over the last decades led to strategies to improve image quality. Two of these techniques are slice encoding for metal artifact correction (SEMAC) and view angle tilting (VAT). They proved to reduce artifacts, however at the cost of prolonging scanning times [10, 11]. Since artifact severity is highly dependent on implant alloys, these techniques are somehow limited in their capabilities [12]. A further promising approach to reduce susceptibility artifact-related image degradation might be the use of MRI systems with lower field strengths. However, data on susceptibility artifacts in low-field MRI below 1.0-T field strength is limited [13].

Finally, the impact of implant-related artifacts on diagnostic accuracy and clinical decision making might differ between radiologists and orthopedic surgeons who review images for preoperative planning. Assessment of artifact severity and image quality thus remains challenging and is performed either qualitatively [11, 14] or quantitatively [15].

The aim of our study was to visually and quantitatively investigate hip implant-related metal artifacts of three distinct implant alloys on a newly introduced 0.55-T scanner system in comparison to images acquired on 1.5-T and 3-T systems with metal artifact reduction sequences (MARS) from clinical routine.

Methods

Approval by the institutional review board as well as informed consent was not required for this prospective experimental phantom study.

Phantom

Phantom measurements were performed using three identically shaped femoral components from total hip arthroplasty: Müller Straight Stem (size 10, length 140 mm, width 12.6 mm, offset 40.8 mm, neck length 39.4 mm) made of three different alloys: titanium (Ti), cobalt-chromium (Co-Cr), and stainless steel (Fe-Cr). Implants were bedded on a foam padding (polyurethane) in a water phantom (Fig. 1a). Identical placement of all femoral components within the water phantom for each scan was ensured through markers drawn on the foam padding.

MRI protocol

Imaging was performed on three different systems from the same manufacturer (Siemens Healthineers, Erlangen, Germany): a 0.55-T Magnetom Free.Max; a 1.5-T Magnetom Avanto FIT; a 3-T Magnetom Prisma. Technical specifications of scanners are summarized in Table 1.

Each femoral component was scanned separately using an optimized imaging protocol with metal artifact reduction sequences (MARS) from clinical routine. Pulse sequences included coronal T2-weighted turbo spin-echo (TSE), coronal turbo inversion-recovery magnitude (TIRM), axial T1-weighted TSE, axial TIRM, and sagittal T1-weighted TSE. Pulse sequence parameters are summarized in Table 2. Six-channel receiving flex coils were used in combination with receiving spine coils integrated in the scanners' patient tables.

Visual and quantitative artifact assessment

Artifact severity was visually assessed on all pulse sequences at two time points by a fellowship-trained musculoskeletal radiologist with 8 years of experience, a musculoskeletal radiology fellow with 2 years of experience and an orthopedic surgeon with 19 years of experience in hip surgery. A 7-point Likert scale (0 = no artifacts, 1 = minimal artifacts, 2 = mild artifacts, 3 = moderate artifacts, 4 = severe artifacts, 5 = very severe artifacts, 6 = extremely severe artifacts) was used for assessment [16]. Readers were blinded to pulse sequences, field strengths, alloys, and other readers' assessments. Four weeks were allotted between the two reading sessions to reduce recall bias. The order of the pulse sequences was varied by random computer sorting for the second reading, and each reader was blinded to its prior interpretation.

Visual assessment of artifact severity was performed on nine slices for each implant at each field strength: one slice at the center of the femoral component for both coronal acquisitions (coronal T2-weighted TSE and T2-weighted TSE TIRM; Fig. 1b), one slice at the center of the femoral component for the sagittal acquisition

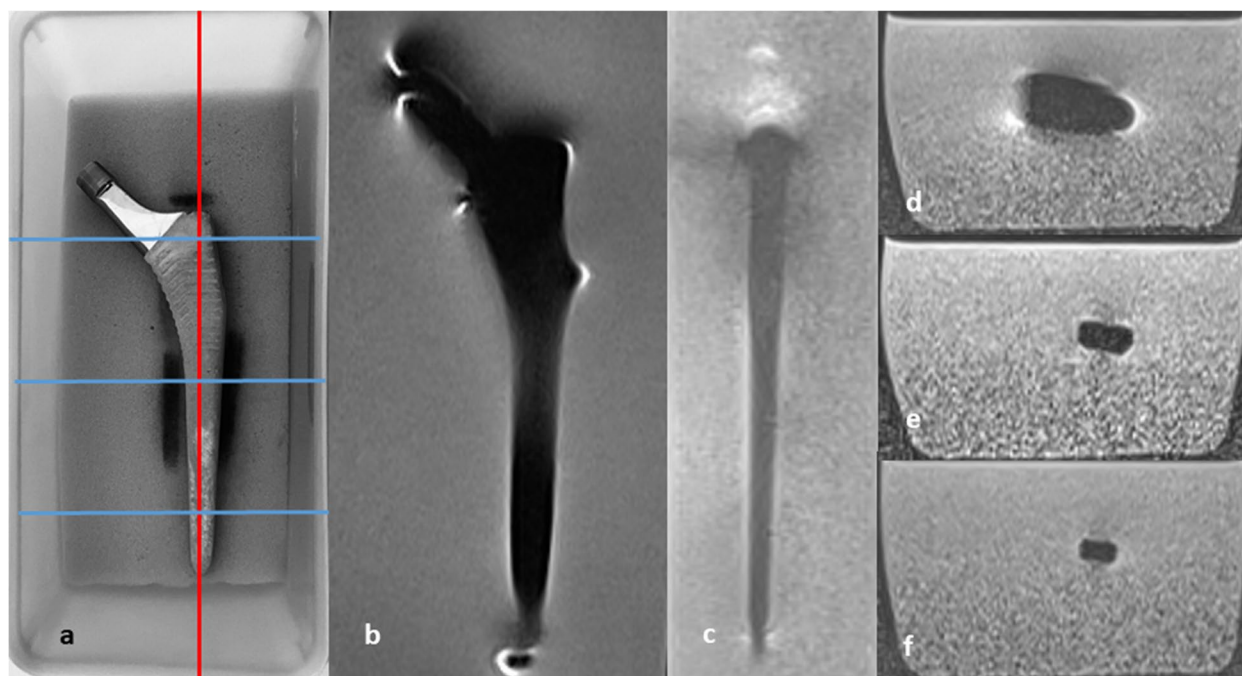


Fig. 1 Femoral component on a foam pad within a water phantom (a). Corresponding slice positions in coronal (b), sagittal (c; red line in a), and three axial planes (d, e, f; blue lines in a) predefined as reference for visual and quantitative assessment

Table 1 Specifications of 0.55-T, 1.5-T, and 3-T scanner systems

	Bore width (cm)	Field strength (T)	Gradient amplitude (mT/m)	Slew rate (T/m/s)
Magnetom Free.Max	80	0.55	26	45
Magnetom Avanto FIT	60	1.50	45	200
Magnetom Prisma	60	3.00	80	200

(sagittal T1-weighted TSE; Fig. 1c) and three slices located in the proximal, middle, and distal portion of the femoral component for the two axial acquisitions (axial T2-weighted TSE TIRM and T1-weighted TSE; Fig. 1d–f). In total, 81 slices (3 alloys \times 3 field strengths \times 9 slices) were assessed twice by each reader.

Quantitative assessment of artifact severity was performed on the same nine slices per implant and field strength through calculation of the coefficient of variation. Furthermore, a normalized signal intensity map was calculated for each slice (Fig. 2) and the fractions of voxels within the water phantom lying 10% (p10), 25% (p25), and 50% (p50) above or below the mean signal intensity of an automatically defined control region of interest were determined (Fig. 3).

Statistical analysis

Interreader and intrareader agreement were determined by interclass and intraclass correlation coefficient (ICC).

ICC values were interpreted as poor (ICC < 0.40), fair (ICC = 0.40–0.59), good (ICC = 0.60–0.74), and excellent (ICC = 0.75–1.0) [17]. Statistical differences between Likert scores were evaluated using the Wilcoxon signed-rank test. Correlation between Likert scores from visual assessment and parameters from quantitative assessment was determined using Spearman's rho. Coefficient values were categorized as weak ($r \leq 0.30$), moderate ($r = 0.31–0.69$), and strong ($r = 0.70–1.0$) [18]. p values < 0.05 were considered to represent a statistically significant difference.

Results

Intrareader and interreader agreement

Intrareader agreement between the two reading sessions was excellent for all three readers (reader 1, ICC 0.89; reader 2, ICC 0.92; reader 3, ICC 0.78). The interreader agreement between the two radiologists (reading 1, ICC 0.76; reading 2, ICC 0.82; overall, ICC = 0.82; Fig. 4a) and the interreader agreement between the two radiologists and the orthopedic surgeon (reading 1, 0.66–0.68; reading 2, 0.80–0.82; overall, ICC 0.74–0.77) were good to excellent.

Visual artifact assessment

Artifact severity was scored lowest for the femoral component made of Ti at 0.55 T (mean Likert score: 2.46 ± 1.03). Likewise, artifact severities of the Ti implant were

Table 2 Imaging protocols and pulse sequence parameters for 0.55-T, 1.5-T and 3-T scanner systems

Field strength	Plane	Sequence	TR (ms)	TE (ms)	T1 (ms)	BW (Hz/pixel)	FOV (mm)	Matrix	ST (mm)	TA (min)
0.55 T	Coronal	T2 TSE TIRM	4,440	35	100	299	220 × 220	134 × 192	3.5	02:48
	Coronal	T2 TSE	3,220	77	-	434	220 × 220	224 × 320	3.5	02:21
	Axial	T2 TSE TIRM	4,260	25	100	302	220 × 220	192 × 240	5	04:58
	Axial	T1 TSE	517	9.4	-	401	220 × 220	213 × 304	5	03:40
	Sagittal	T1 TSE	517	9.4	-	401	220 × 220	213 × 304	5	03:40
1.5 T	Coronal	T2 TSE TIRM	4,000	34	150	455	220 × 220	192 × 256	3.5	01:48
	Coronal	T2 TSE	3,400	73	-	430	220 × 220	358 × 448	3.5	01:25
	Axial	T2 TSE TIRM	5,210	54	150	400	180 × 180	224 × 320	5	03:33
	Axial	T1 TSE	661	9.5	-	305	200 × 200	218 × 256	5	05:44
	Sagittal	T1 TSE	596	8.5	-	460	220 × 220	256 × 320	5	02:32
3 T	Coronal	T2 TSE TIRM	4,800	42	210	505	240 × 240	240 × 320	3.5	01:36
	Coronal	T2 TSE	4,500	73	-	505	220 × 220	224 × 320	3.5	01:30
	Axial	T2 TSE TIRM	4,200	39	200	500	180 × 180	205 × 256	5	02:06
	Axial	T1 TSE	687	17	-	520	200 × 200	320 × 320	5	02:53
	Sagittal	T1 TSE	600	9.3	-	520	240 × 240	384 × 384	5	02:32

BW Bandwidth, FOV Field of view, ST Slice thickness, T1 T1-weighted, T2 T2-weighted, TA Acquisition time, TE Echo time, TI Inversion time, TIRM Turbo inversion-recovery magnitude, TR Repetition time, TSE Turbo spin-echo

rated lower than those of the other alloys both at 1.5 T (2.91 ± 1.16 for Ti *versus* 3.93 ± 1.46 for Co-Cr and 4.11 ± 1.63 for Fe-Cr; $p = 0.151$ and $p = 0.091$, respectively) and at 3 T (3.72 ± 0.91 for Ti *versus* 4.67 ± 1.05 for Co-Cr and 5.17 ± 1.06 for Fe-Cr; $p = 0.060$ and $p < 0.001$, respectively).

Artifact severities of all three alloys were scored significantly lower at 0.55 T compared to 3 T (e.g., Ti implant 2.46 ± 1.03 *versus* 3.72 ± 0.91 , $p < 0.001$). Also at 1.5 T, the artifact severity scores determined by the three readers were significantly lower for Ti than those at 3 T (e.g., Ti implant 2.91 ± 1.16 *versus* 3.72 ± 0.91 , $p = 0.043$). Visual

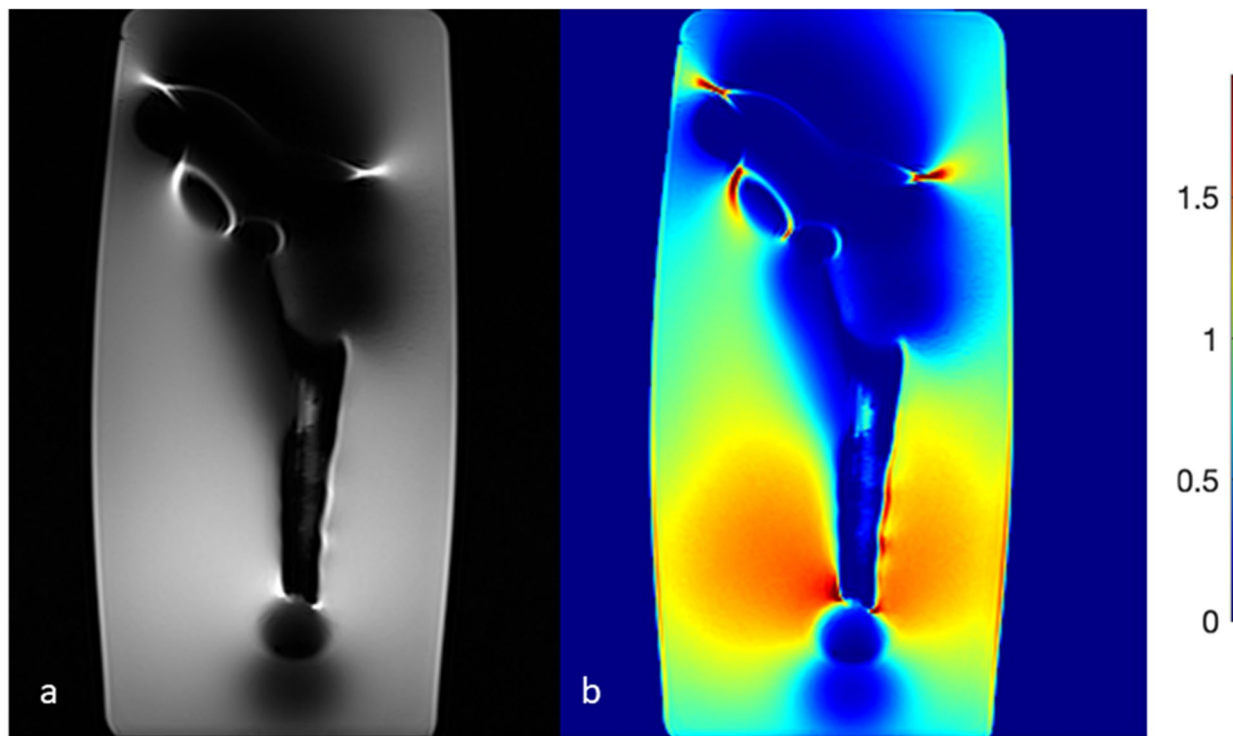


Fig. 2 Coronal T2-weighted turbo spin-echo image of an implant (Fe-Cr) at 1.5 T (a) with the normalized signal intensity on the right (b)

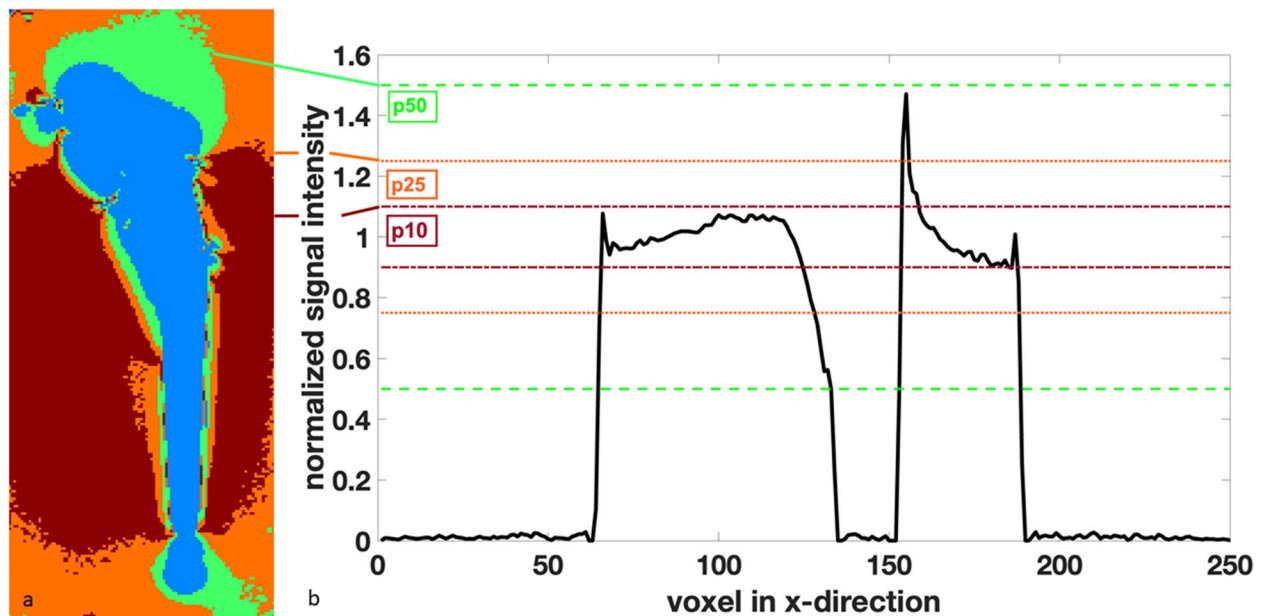


Fig. 3 Scheme of the fractions of voxel within a 10%, 25%, and 50% limit above or below the mean signal intensity (a). Corresponding signal curve along the x-axis at the middle of the shaft with visualization of the fractions p10, p25, and p50 (b). See text (in the “Methods” section) for explanation of p10, p25, and p50

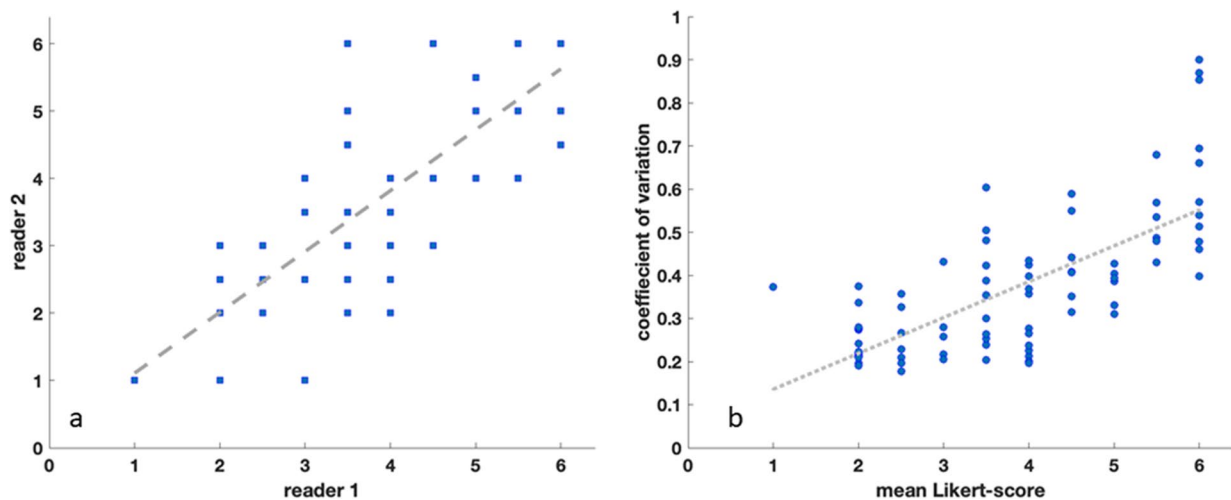


Fig. 4 Scatter plots showing the correlation of reader 1 and 2 (a) and the correlation of mean Likert scores and coefficients of variation (b)

assessment however did not reveal statistically significant differences between artifact severities at 0.55 T and 1.5 T (e.g., Ti implant 2.46 ± 1.03 versus 2.91 ± 1.16 , $p = 0.451$).

While artifacts of the Co-Cr implant were scored slightly less severe than those of stainless steel implants at all three field strengths, the differences were not statistically significant (e.g., at 3T, 4.67 ± 1.05 for Co-Cr versus 5.17 ± 1.06 for Fe-Cr, $p = 0.254$). All Likert scores and p values are listed in Table 3.

Quantitative artifact assessment

The lowest artifact intensities were measured for the femoral component made of Ti at 1.5 T and 0.55 T with a coefficient of variation of 0.28 ± 0.08 and 0.31 ± 0.06 , respectively. Similarly, quantitative artifact assessment showed no statistically significant differences for the two other alloys at 0.55 T and 1.5 T: Co-Cr 0.35 ± 0.09 versus 0.35 ± 0.10 and Fe-Cr 0.37 ± 0.12 versus 0.36 ± 0.16 ($p \geq 0.059$).

Table 3 Likert scores overall and per reader for each distinct alloy at 0.55T, 1.5T, and 3T

		Reader 1	Reader 2	Reader 3	Overall	Significant p values
0.55 T	Titanium	2.33 ± 0.90	1.89 ± 0.83	3.17 ± 1.10	2.46 ± 1.03 (*,**,+)	*: p < 0.01
	Cobalt-chromium	3.67 ± 0.43	3.94 ± 0.85	4.44 ± 0.92	4.02 ± 0.51 (*,++)	+: p = 0.08
	Stainless steel	4.33 ± 0.94	3.50 ± 1.97	4.78 ± 0.87	4.20 ± 1.11 (**,+++)	++: p = 0.49
1.5 T	Titanium	2.78 ± 1.15	2.94 ± 1.13	3.00 ± 1.44	2.91 ± 1.16 (-)	+++: p = 0.042
	Cobalt-chromium	3.83 ± 1.44	4.00 ± 1.48	3.94 ± 1.65	3.93 ± 1.46	o: p = 0.07
	Stainless steel	3.94 ± 1.79	4.22 ± 1.56	4.17 ± 1.64	4.11 ± 1.63	
3 T	Titanium	4.00 ± 1.12	3.17 ± 1.09	4.00 ± 1.12	3.72 ± 0.91 (o,+,-)	
	Cobalt-chromium	4.61 ± 1.14	4.56 ± 1.36	4.83 ± 1.12	4.67 ± 1.05 (+,++)	
	Stainless steel	5.22 ± 1.00	5.00 ± 1.32	5.28 ± 0.97	5.17 ± 1.06 (o,+,+++)	

Data are given as mean ± standard deviation. Pairwise significant differences of the mean score existed between titanium at 0.55 T and cobalt-chromium/stainless steel at 0.55 T (***), titanium at 0.55 T and titanium at 3 T (+), titanium at 1.5 T and titanium at 3 T (-), cobalt-chromium at 0.55 T and cobalt-chromium at 3 T (++), stainless steel at 0.55 T and stainless steel at 3 T (+++), and between Titanium at 3 T and stainless steel at 3 T (-)

Table 4 Coefficient of variation and fraction of voxels within a 10% (p10), 25% (p25), and 50% (p50) limit above or below mean signal intensity within the phantom at 0.55 T, 1.5 T, and 3 T. No statistically significant differences exist

		CoV	p10	p25	p50
0.55 T	Titanium	0.31 ± 0.06	0.41 ± 0.11	0.74 ± 0.10	0.90 ± 0.04
	Cobalt-chromium	0.35 ± 0.09	0.37 ± 0.15	0.69 ± 0.14	0.86 ± 0.06
	Stainless steel	0.37 ± 0.12	0.38 ± 0.10	0.69 ± 0.11	0.85 ± 0.09
1.5 T	Titanium	0.28 ± 0.08	0.55 ± 0.07	0.82 ± 0.05	0.91 ± 0.04
	Cobalt-chromium	0.35 ± 0.10	0.46 ± 0.16	0.73 ± 0.14	0.85 ± 0.09
	Stainless steel	0.36 ± 0.16	0.44 ± 0.16	0.70 ± 0.19	0.83 ± 0.14
3 T	Titanium	0.34 ± 0.13	0.30 ± 0.13	0.66 ± 0.18	0.86 ± 0.12
	Cobalt-chromium	0.43 ± 0.19	0.31 ± 0.16	0.59 ± 0.24	0.75 ± 0.21
	Stainless steel	0.62 ± 0.19	0.25 ± 0.15	0.47 ± 0.24	0.64 ± 0.20

CoV Coefficient of variation

Strongest artifacts were observed for the femoral component made of stainless steel at 3 T with a coefficient of variation of 0.62 ± 0.19. The fraction of voxels lying within a threshold of 10%, 25%, and 50% above or below mean signal intensity were 0.25 ± 0.15, 0.47 ± 0.20, and 0.64 ± 0.20, respectively.

Artifacts were less severe for Ti and Co-Cr alloys than for implants made of stainless steel at all three field strengths (Table 4, Figs. 5 and 6).

Correlation between visual and quantitative assessment

There was a strong positive linear correlation between the calculated coefficients of variation and the three readers' Likert scores from visual artifact severity assessment

($r = 0.87$; $p = 0.005$, Fig. 4b). Strong negative linear correlations were seen for both the 25% and 50% thresholds of voxels lying above or below mean signal intensity and the Likert scores (p25, $r = -0.84$, $p = 0.005$; p50, $r = -0.85$, $p = 0.007$). Moderate negative correlation was observed for p10 and visual assessments' Likert scores ($r = -0.73$; $p = 0.032$)

Discussion

The aim of our study was to visually and quantitatively evaluate the influence of field strength and implant alloys on susceptibility-induced artifacts in hip implant imaging. Although artifact severities were scored lowest for Ti implants at 0.55 T in terms of absolute values (mean Likert score: 2.46 ± 1.03), visual assessment showed no significant differences between imaging at 0.55 T and 1.5 T (e.g., for Ti implants 2.46 ± 1.03 versus 2.91 ± 1.16, $p = 0.451$). Strong intrareader agreement (ICC 0.78–0.92) and strong to moderate interreader agreement (ICC 0.74–0.77) were found between the two subspecialized musculoskeletal radiologists and the orthopedic surgeon during visual assessment of image quality. Their ratings strongly correlated with the parameters used for quantitative evaluation of artifact intensities, i.e., with the coefficient of variation ($r = 0.87$; $p = 0.005$). To our best knowledge, this is the first study which has been performed on a commercially available, non-experimental 0.55-T scanner.

Both visually and quantitatively, artifacts of Ti alloys were least severe, while those of stainless steel implants were strongest at all three field strengths. This is in accordance with recently published literature [12, 19]. Artifacts for all three alloys were rated lower at 0.55 T and 1.5 T compared to 3 T during visual assessment. Although artifacts were evaluated slightly less severe at 0.55 T compared to 1.5 T for some alloys (e.g., for Ti 2.46

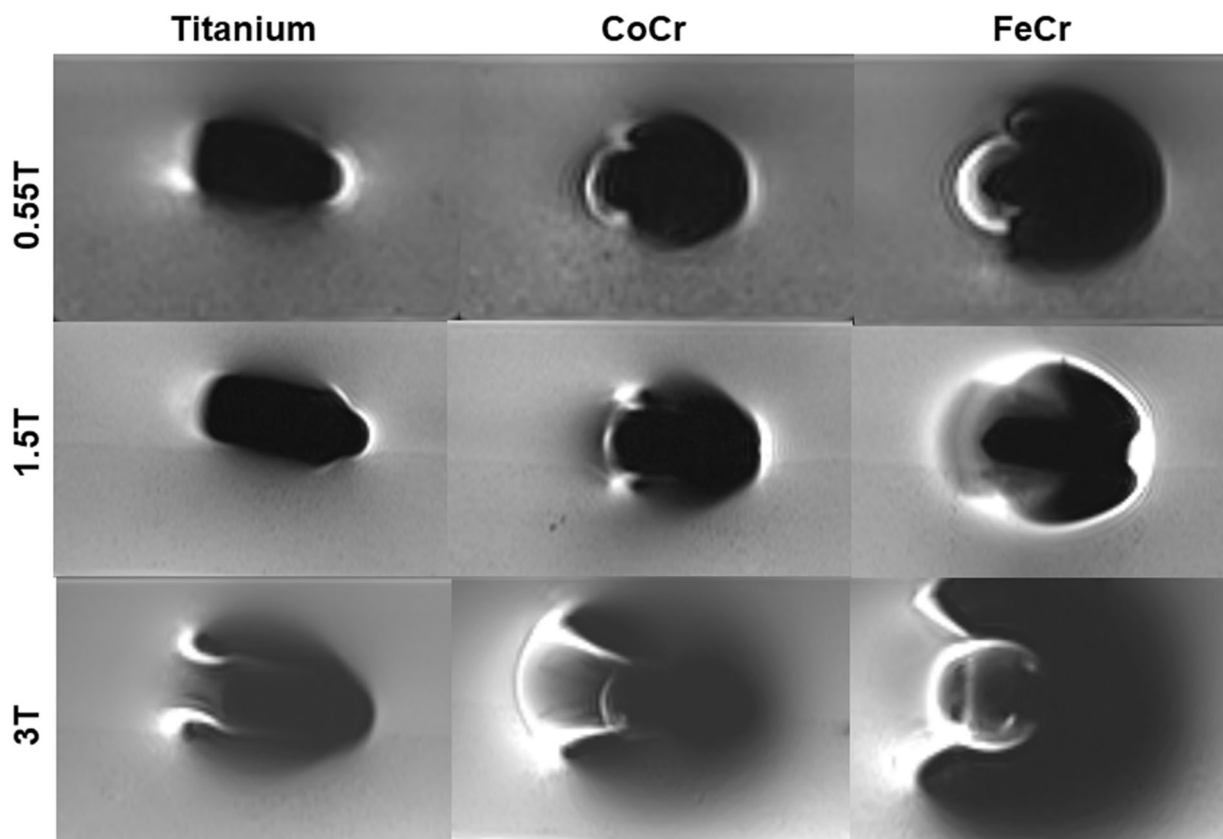


Fig. 5 Axial slices through the femoral components made of three different alloys at 0.55 T, 1.5 T, and 3 T. Artifacts are lowest for Ti and increase with higher magnetic field strength for all three alloys

± 1.03 versus 2.91 ± 1.16), these differences were not statistically significant.

During quantitative artifact assessment, the lowest artifact intensities were observed for the Ti implant at 1.5 T. This contrasts previous investigations, *e.g.*, the study of Matsuura et al., who demonstrated less artifacts for neurosurgical biomaterials at 0.5 T compared to 1.5 T and 3 T [20, 21]. This discrepancy might be explained by substantial differences in technical specifications of the scanner systems used. Gradients of our commercially available 0.55-T scanner system were lower compared to the experimental 0.5-T scanner system used by Matsuura et al., as well as compared to clinically established 1.5-T and 3-T scanner systems (Table 1). Furthermore, our 0.55-T system operates with a substantially larger bore width of 80 cm (compared to 60 cm for the 1.5-T and 3-T scanner systems) to improve patient comfort [22].

Our study has several limitations. For imaging at 1.5 T and 3 T, we used optimized pulse sequences from clinical routine, which were not further amended for scanning at 0.55 T, as the primary aim of our investigation was to evaluate the influence of magnetic field strength alone. With addition optimization of pulse sequence

parameters, susceptibility artifacts at 0.55 T might be further reduced. Especially the effects of advanced imaging techniques such as VAT or SEMAC, which are known to improve image quality at 1.5 and 3 T, have to be evaluated at 0.55 T [15]. In addition to that, a phantom-based evaluation of susceptibility-induced artifacts only allows to forecast which artifacts might have to be expected with *in vivo* scanning. Investigations on how these artifacts actually impact the evaluation of distinct surrounding anatomic structures must include prospective scanner-scanner comparison studies in human subjects. Although a new objectifiable and reproducible method for artifact quantification was created, which has a good agreement with the subjective ratings, the influence of factors such as instrument-related specifications (for example, bore width or homogeneity of the B_0 field) remains unclear. In particular, an increasing field causes a shortening wavelength and results in a nonuniformity of intensity profiles. Through the respective normalization to the image to be evaluated, an attempt was made to objectify this as best as possible. Finally, visual perception and evaluation of artifacts by the individual readers is highly subjective and might differ between radiologists and other clinicians.

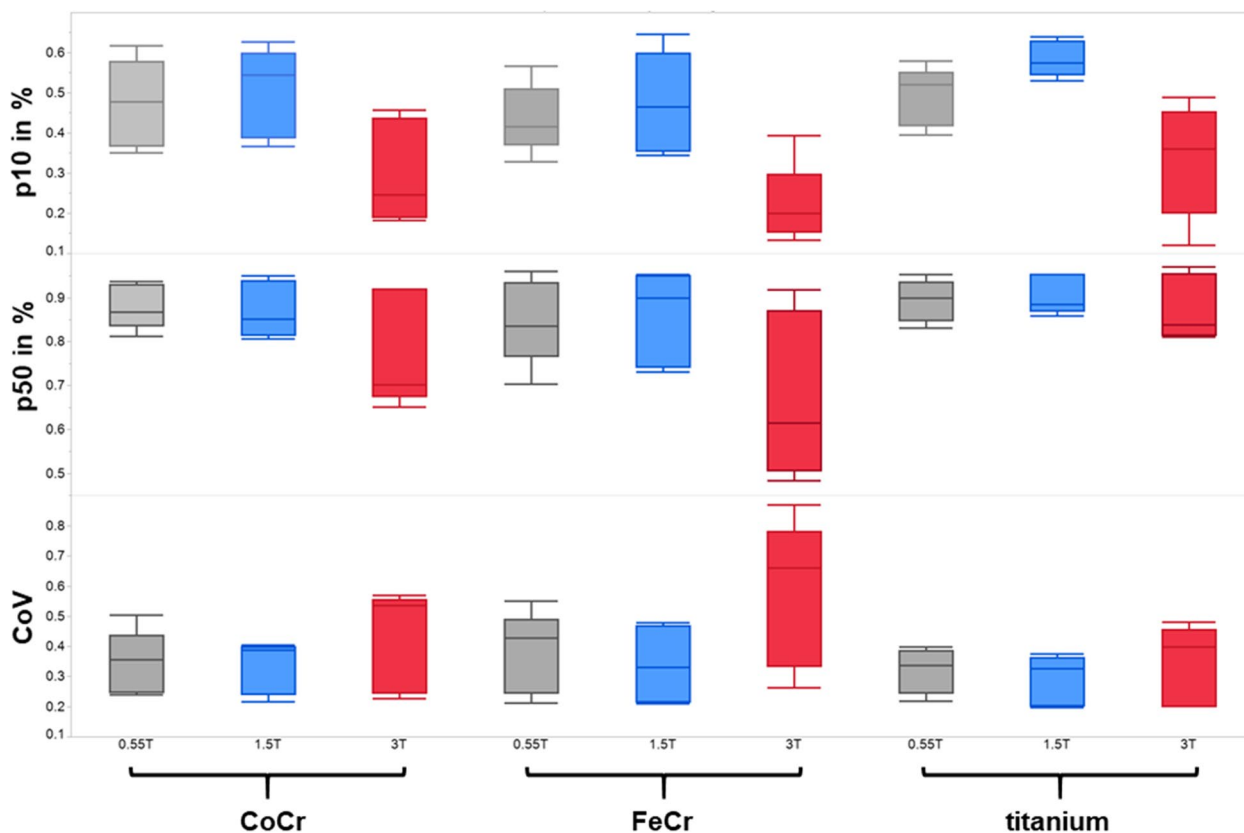


Fig. 6 Overview of the quantitative parameters p10, p50, and coefficients of variation (CoV) for the different field strengths and alloys. See text (in the “Methods” section) for explanation of p10, p25, and p50

Therefore, visual assessment was performed both by two musculoskeletal radiologists and one orthopedic surgeon and quantitative parameters were used to correlate with visual evaluation.

In conclusion, our results demonstrate that susceptibility-induced artifacts of hip implants at a commercially available 0.55-T scanner are comparable to MARS imaging at 1.5 T despite an inferior gradient system and larger bore width. The additional use of advanced imaging techniques and reconstruction mechanisms [19, 23] may further reduce artifacts at 0.55 T. Current limitations of metal implant imaging at higher field strengths, *i.e.*, specific absorption rates and tissue heating [24, 25] might also be overcome with low field MRI at 0.55 T.

Abbreviations

Co-Cr	Cobalt-chromium
Fe-Cr	Iron-chromium (stainless steel)
ICC	Intra/inter-class correlation coefficient
MRI	Magnetic resonance imaging
MARS	Metal artifact reduction sequences
p10	Fractions of voxels within the water phantom lying 10%
p25	Fractions of voxels within the water phantom lying 25%
p50	Fractions of voxels within the water phantom lying 50%

SEMAC	Slice encoding for metal artifact correction
Ti	Titanium
TIRM	Turbo inversion-recovery magnitude
TSE	Turbo spin-echo
VAT	View angle tilting

Authors' contributions

HCB made substantial contributions to the conception, design of the work, the acquisition, analysis, interpretation of the data, and the creation of new software used in the work and has approved the submitted version. HCB has agreed both to be personally accountable for the author's own contributions and to ensure that questions related to the accuracy or integrity of any part of the work, even ones in which the author was not personally involved, are appropriately investigated, resolved, and the resolution documented in the literature. JV made substantial interpretation of the data and has approved the submitted version. JV has agreed both to be personally accountable for the author's own contributions and to ensure that questions related to the accuracy or integrity of any part of the work, even ones in which the author was not personally involved, are appropriately investigated, resolved, and the resolution documented in the literature. MC made substantial contributions to the conception, design of the work, and the acquisition and has approved the submitted version. MC has agreed both to be personally accountable for the author's own contributions and to ensure that questions related to the accuracy or integrity of any part of the work, even ones in which the author was not personally involved, are appropriately investigated, resolved, and the resolution documented in the literature. TJW made substantial contributions to design of the work and the acquisition and has approved the submitted version. TJW has agreed both to be personally accountable for the author's own contributions and to ensure that questions related to the accuracy or integrity of any part of the work,

even ones in which the author was not personally involved, are appropriately investigated, resolved, and the resolution documented in the literature. BS made substantial contributions to the conception and has approved the submitted version. BS has agreed both to be personally accountable for the author's own contributions and to ensure that questions related to the accuracy or integrity of any part of the work, even ones in which the author was not personally involved, are appropriately investigated, resolved, and the resolution documented in the literature. MB made substantial contributions to the conception and has approved the submitted version. MB has agreed both to be personally accountable for the author's own contributions and to ensure that questions related to the accuracy or integrity of any part of the work, even ones in which the author was not personally involved, are appropriately investigated, resolved, and the resolution documented in the literature. BK made substantial contributions to the analysis and has approved the submitted version. BK has agreed both to be personally accountable for the author's own contributions and to ensure that questions related to the accuracy or integrity of any part of the work, even ones in which the author was not personally involved, are appropriately investigated, resolved, and the resolution documented in the literature. DH made substantial contributions to the conception, design of the work, and the acquisition and has approved the submitted version. DH has agreed both to be personally accountable for the author's own contributions and to ensure that questions related to the accuracy or integrity of any part of the work, even ones in which the author was not personally involved, are appropriately investigated, resolved, and the resolution documented in the literature. The authors read and approved the final manuscript.

Fundings

The authors state that this work has not received any funding.

Availability of data and materials

The datasets used and/or analyzed during the current study are available from the corresponding author on reasonable request.

Declarations

Ethics approval and consent to participate

Institutional Review Board approval was not required because it was a phantom study.

Consent for publication

Not applicable (phantom study).

Competing interests

The authors of this manuscript declare no relationships with any companies, whose products or services may be related to the subject matter of the article.

Received: 6 August 2022 Accepted: 30 December 2022

Published online: 08 February 2023

References

- Kurtz S, Ong K, Lau E, Mowat F, Halpern M (2007) Projections of primary and revision hip and knee arthroplasty in the United States from 2005 to 2030. *J Bone Joint Surg Am* 89:780–785. <https://doi.org/10.2106/JBJS.F.00222>
- Abdelaal MS, Restrepo C, Sharkey PF (2020) Global perspectives on arthroplasty of hip and knee joints. *Orthop Clin North Am* 51:169–176. <https://doi.org/10.1016/j.ocl.2019.11.003>
- Kurtz SM, Lau E, Ong K, Zhao K, Kelly M, Bozic KJ (2009) Future young patient demand for primary and revision joint replacement: national projections from 2010 to 2030. In: *Clinical Orthopaedics and Related Research*. Springer, New York, pp 2606–2612. <https://doi.org/10.1007/s11999-009-0834-6>
- Bonn D (1998) UK patients with hip implants to be reviewed. *Lancet* 351:651. [https://doi.org/10.1016/S0140-6736\(98\)23009-1](https://doi.org/10.1016/S0140-6736(98)23009-1)
- Nawabi DH, Hayter CL, Su EP, et al (2013) Magnetic resonance imaging findings in symptomatic versus asymptomatic subjects following metal-on-metal hip resurfacing arthroplasty. *J Bone Joint Surg Am* 95:895–902. <https://doi.org/10.2106/JBJS.K.01476>
- Chang EY, McAnally JL, Van Horne JR, et al (2012) Metal-on-metal total hip arthroplasty: do symptoms correlate with MR imaging findings? *Radiology* 265:848–857. <https://doi.org/10.1148/radiol.12120852>
- Robinson E, Henckel J, Sabah S, Satchithananda K, Skinner J, Hart A (2014) Cross-sectional imaging of metal-on-metal hip arthroplasties: can we substitute MARS MRI with CT? *Acta Orthop* 85:577–584. <https://doi.org/10.3109/17453674.2014.964618>
- Siddiqui IA, Sabah SA, Satchithananda K, et al (2014) A comparison of the diagnostic accuracy of MARS MRI and ultrasound of the painful metal-on-metal hip arthroplasty. *Acta Orthop* 85:375–382. <https://doi.org/10.3109/17453674.2014.908345>
- Attenberger UI, Biber S, Wichtmann BD (2020) Technological advances of magnetic resonance imaging in today's health care environment. *Invest Radiol* 55:531–542. <https://doi.org/10.1097/RLI.0000000000000678>
- Ai T, Padua A, Goerner F, et al (2012) SEMAC-VAT and MSVAT-SPACE sequence strategies for metal artifact reduction in 1.5 T magnetic resonance imaging. *Invest Radiol* 47:267–276. <https://doi.org/10.1097/RLI.0b013e318240a919>
- Lee YH, Lim D, Kim E, Kim S, Song H-T, Suh J-S (2013) Usefulness of slice encoding for metal artifact correction (SEMAC) for reducing metallic artifacts in 3-T MRI. *Magn Reson Imaging* 31:703–706. <https://doi.org/10.1016/j.mri.2012.11.004>
- Filli L, Jud L, Luechinger R, et al (2017) Material-dependent implant artifact reduction using SEMAC-VAT and MAVRIC: A prospective MRI phantom study. *Invest Radiol* 52:381–387. <https://doi.org/10.1097/RLI.0000000000000351>
- Runge VM, Heverhagen JT (2020) The next generation—advanced design low-field MR systems. *Magnetom FLASH. Free Max Special Issue*:11–19. https://marketing.webassets.siemens-healthineers.com/fe3039b55a19dbff/6b2fa4ff0b07/Runge_Heverhagen_Advanced_Design_Low-field_MRI_RSNA2020.pdf
- Chang SD, Lee MJ, Munk PL, Janzen DL, MacKay A, Xiang Q-S (2001) MRI of spinal hardware: comparison of conventional T1-weighted sequence with a new metal artifact reduction sequence. *Skeletal Radiol* 30:213–218. <https://doi.org/10.1007/s002560100331>
- Lee MJ, Janzen DL, Munk PL, MacKay A, Xiang Q-S, McGowen A (2001) Quantitative assessment of an MR technique for reducing metal artifact: application to spin-echo imaging in a phantom. *Skeletal Radiol* 30:398–401. <https://doi.org/10.1007/s002560100332>
- Finstad K (2010) Response interpolation and scale sensitivity: evidence against 5-point scales. *J Usability Stud* 5:104–110. <https://doi.org/10.5555/2835434.2835437>
- Hallgren KA (2012) Computing inter-rater reliability for observational data: an overview and tutorial. *Tutor Quant Methods Psychol* 8:23. <https://doi.org/10.20982/tqmp.08.1.p023>
- Ratner B (2009) The correlation coefficient: Its values range between +1/– 1, or do they? *J Target Measure Anal Market* 17:139–142. <https://doi.org/10.1057/jt.2009.5>
- Jungmann PM, Bensler S, Zingg P, Fritz B, Pfirrmann CW, Sutter R (2019) Improved visualization of juxtaarthrotic tissue using metal artifact reduction magnetic resonance imaging: experimental and clinical optimization of compressed sensing SEMAC. *Invest Radiol* 54:23–31. <https://doi.org/10.1097/RLI.0000000000000504>
- Matsuura H, Inoue T, Ogasawara K, et al (2005) Quantitative analysis of magnetic resonance imaging susceptibility artifacts caused by neurosurgical biomaterials: comparison of 0.5, 1.5, and 3.0 Tesla magnetic fields. *Neurol Med Chir (Tokyo)* 45:395–399. <https://doi.org/10.2176/nmc.45.395>
- Khodarahmi I, Brinkmann IM, Lin DJ, et al (2022) New-generation low-field magnetic resonance imaging of hip arthroplasty implants using slice encoding for metal artifact correction: first in vitro experience at 0.55 T and comparison with 1.5 T. *Invest Radiol*. <https://doi.org/10.1097/RLI.0000000000000866>
- Iwan E, Yang J, Enders J, Napp AE, Rief M, Dewey M (2020) Patient preferences for development in MRI scanner design: a survey of claustrophobic patients in a randomized study. *Eur Radiol*. <https://doi.org/10.1007/s00330-020-07060-9>
- Ranzini MBM, Groothuis I, Kläser K, et al (2020) Combining multimodal information for metal artefact reduction: an unsupervised deep learning framework. In: 2020 IEEE 17th International Symposium on Biomedical

Imaging (ISBI). IEEE, pp 600–604. <https://doi.org/10.48550/arXiv.2004.09321>

24. Khodarahmi I, Rajan S, Sterling R, Koch K, Kirsch J, Fritz J (2021) Heating of hip arthroplasty implants during metal artifact reduction MRI at 1.5- and 3.0-T field strengths. *Invest Radiol* 56:232–243. <https://doi.org/10.1097/RLI.0000000000000732>
25. Wang ZW, Lin JC, Mao WH, Liu WZ, Smith MB, Collins CM (2007) SAR and temperature: simulations and comparison to regulatory limits for MRI. *J Magn Reson Imaging* <https://doi.org/10.1002/jmri.20977>

Publisher's Note

Springer Nature remains neutral with regard to jurisdictional claims in published maps and institutional affiliations.

Submit your manuscript to a SpringerOpen[®] journal and benefit from:

- ▶ Convenient online submission
- ▶ Rigorous peer review
- ▶ Open access: articles freely available online
- ▶ High visibility within the field
- ▶ Retaining the copyright to your article

Submit your next manuscript at ▶ [springeropen.com](https://www.springeropen.com)
